Carcinogenesis vol.34 no.7 pp.1487–1496, 2013
doi:10.1093/carcin/bgt099
Advance Access publication March 23, 2013

Anthraquinone emodin inhibits human cancer cell invasiveness by antagonizing P2X7 receptors

Bilel Jelassi[1], Monique Anchelin[2], Julie Chamouton[1], María Luisa Cayuela[2], Lucie Clarysse[1], Junying Li[3], Jacques Goré[1], Lin-Hua Jiang[1,4] and Sébastien Roger[1,5,*]

[1]Inserm U1069 Nutrition, Growth and Cancer, Université François-Rabelais de Tours, 10 Boulevard Tonnellé, 37032 Tours, France, [2]Telomerase, Cancer and Aging Group, University Hospital "Virgen de la Arrixaca"-FFIS, Carretera Palmar, 30120 Murcia, Spain, [3]Department of Biophysics, School of Physics and Key Laboratory of Bioactive Materials of Education Ministry, Nankai University, Tianjin 300071, China, [4]School of Biomedical Sciences, Faculty of Biological Sciences, University of Leeds, Leeds LS2 9JT, United Kingdom and [5]Département de Physiologie Animale, UFR Sciences et Techniques, Université François-Rabelais de Tours, 10 Boulevard Tonnellé, 37032 Tours, France

*To whom correspondence should be addressed. Tel: +33 2 47 36 61 30;
Fax: +33 2 47 36 62 26;
Email: sebastien.roger@univ-tours.fr
Correspondence may also be addressed to Lin-Hua Jiang.
Tel: +44 113 3434231;
Email: l.h.jiang@leeds.ac.uk

The adenosine 5′-triphosphate (ATP)-gated Ca^{2+}-permeable channel P2X7 receptor (P2X7R) is strongly upregulated in many tumors and cancer cells, and has an important role in cancer cell invasion associated with metastases. Emodin (1,3,8-trihydroxy-6-methylanthraquinone) is an anthraquinone derivative originally isolated from *Rheum officinale* Baill known for decades to possess anticancer properties. In this study, we examined the effects of emodin on P2X7R-dependent Ca^{2+} signaling, extracellular matrix degradation, and *in vitro* and *in vivo* cancer cell invasiveness using highly aggressive human cancer cells. Inclusion of emodin at doses ≤10 µM in cell culture had no or very mild effect on the cell viability. ATP elicited increases in intracellular Ca^{2+} concentration were reduced by 35 and 60% by 1 and 10 µM emodin, respectively. Emodin specifically inhibited P2X7R-mediated currents with an IC_{50} of 3 µM and did not inhibit the currents mediated by the other human P2X receptors heterologously expressed in human embryonic kidney (HEK293T) cells. ATP-induced increase in gelatinolytic activity, in cancer cell invasiveness *in vitro* and in cell morphology changes were prevented by 1 µM emodin. Furthermore, such ATP-evoked effects and inhibition by emodin were almost completely ablated in cancer cells transfected with P2X7R-specific small interfering RNA (siRNA) but not with scrambled siRNA. Finally, the *in vivo* invasiveness of the P2X7R-positive MDA-MB-435s breast cancer cells, assessed using a zebrafish model of micrometastases, was suppressed by 40 and 50% by 1 and 10 µM emodin. Taken together, these results provide consistent evidence to indicate that emodin inhibits human cancer cell invasiveness by specifically antagonizing the P2X7R.

Introduction

Epithelial cancers, and principally breast and lung cancers, represent the major causes of death by cancer worldwide (1). The high mortality of the cancerous disease mainly results as a consequence of metastasis appearance and growth. Metastases occur after invading cancer cells degrade and migrate through the extracellular matrix (ECM) and reach the lymph and blood circulation. Therefore, the metastatic progression is likely to depend on the acquisition by cancer cells of a more invasive potency (2). At the time being, there is no specific treatment targeting metastases or preventing metastasis development. Moreover, metastatic cells often exhibit resistance to conventional therapies such as chemotherapies, rendering even more difficult to treat the diseases. Although this clinical reality has been known for years now, the knowledge of molecular and cellular details underlying metastasis remains so far incomplete. In this scenario, increase in the knowledge regarding molecular and cellular mechanisms involved in the development of metastasis and disease progression and discovery of new therapeutic targets should offer a new opportunity to improve clinical practices or develop new strategies for cancer treatments.

Adenosine 5′-triphosphate (ATP) is a well-known intracellular source of energy for all forms of living cells. ATP is also released to the extracellular milieu in both physiological and pathological settings, and initiates signaling pathways through activation of membrane receptors. There are two distinct families of membrane receptors for extracellular nucleotides: the metabotropic G-protein coupled P2Y receptors and the ionotropic ligand-gated cation-permeable channel P2X receptors (3). At the cellular level, these receptors are important regulators of cell activation, proliferation, differentiation, migration and apoptosis, thereby contributing to modulation of several physiological processes. ATP has been found at relatively high concentrations in the tumor microenvironments (4) where it is released from living cancer cells (5) and also from necrotic cells in the perilesional regions of cancers (6), raising the possibility that the purinoreceptors expressed by tumor cells are activated and consequently modulate the tumor growth and metastasis appearance (7,8). Among all receptors, the P2X7 receptor (P2X7R) (9) has drawn increasing attention. It is an intriguing receptor with unique features such as a low ATP sensitivity, no desensitization (10) and remarkable facilitation in response to sustained or repeated exposure to agonist (11,12). The P2X7Rs were initially described as the cytolytic receptors because prolonged activation induced cell death (13,14). The P2X7Rs in immune cells have been extensively studied; their activation is crucial for initiation of the inflammatory signaling cascade through activation of the inflammasome that processes and releases important pro-inflammatory cytokines such as interleukin-1β (15,16) and fever-inducing prostaglandin E2 (17). As such, the P2X7Rs have emerged as an interesting target for developing therapeutics for treatment of inflammatory diseases (18). Studies have recently shown that expression of the P2X7R in several tumors, including chronic lymphocyte leukemia, melanoma, neuroblastoma, prostate, breast and thyroid cancers, is substantially upregulated or higher compared with normal tissues (5,19–25), leading to the proposal of P2X7Rs as an early biomarker for cancer (25,26). Contrarily to the initial assumptions, the P2X7R activity has been shown to be responsible for antiapoptotic effects (24), or for sustaining both cancer cell (5,27) and tumor growth *in vivo* (28). We have recently reported that the P2X7Rs are highly expressed and fully functional in the highly invasive human breast cancer cells MDA-MB-435s (29); activation of the P2X7Rs did not induce cancer cell death but was responsible for the acquisition of a pro-migratory phenotype by cancer cells and enhanced cancer cell invasiveness *in vitro* and *in vivo*, through degradation of the ECM (29). Therefore, the use of P2X7R antagonists may represent a new approach to reduce the development of cancer metastases and improve the efficacy of conventional treatments (8).

Although combinatorial chemistry has emerged as an important part of the medicinal chemistry for production of new drugs, active compounds have been and are still discovered from traditional remedies prepared from plants and other natural sources. Once identified,

Abbreviations: ATP, adenosine 5′-triphosphate; DMEM, Dulbecco's modified Eagle's medium; DMSO, dimethyl sulfoxide; ECM, extracellular matrix; FCS, fetal calf serum; mRNA, messenger RNA; PBS, phosphate-buffered saline; PSS, physiological saline solution; P2X7R, P2X7 receptor; siRNA, small interfering RNA; ZF, zebrafish.

such active compound could represent a good starting point for drug discovery. Emodin (1,3,8-trihydroxy-6-methylanthraquinone), isolated from the rhubarb *Rheum officinale* Baill that has been used in Chinese traditional herbal medicine for centuries, is an anthraquinone derivative and is known to possess anti-inflammatory, immunosuppressive and antitumor properties, despite that the underlying mechanisms are not fully understood (30,31). Recent studies have shown emodin and several other structurally closely related anthraquinone derivatives such as aloe-emodin and rhein to be efficacious in inhibiting melanoma (32) and tongue cancer cell invasiveness (33). Our recent study has demonstrated emodin as a potent rat P2X7R antagonist (34). Therefore, the aim of this study was to investigate whether emodin reduces epithelial (breast and lung) cancer cell invasiveness *in vitro* and *in vivo* through antagonism of the human P2X7R.

Materials and methods

Cells and culture

The human breast (MDA-MB-435s and MDA-MB-468) and non-small cell lung (A549) cancer cells were maintained in Dulbecco's modified Eagle's medium (DMEM), supplemented with 5 and 10% fetal calf serum (FCS), respectively. The immortalized normal mammary epithelial cells MCF-10A were cultured in DMEM/Ham's F-12, 1:1 mix containing 5% horse serum (Invitrogen, Saint Aubin, France), 10 µg/ml insulin, 20 ng/ml epidermal growth factor, 0.5 µg/ml hydrocortisone and 100 ng/ml cholera toxin. Both cell types were originally from the American Type Culture Collection (LGC Promochem, Molsheim, France). The human embryonic kidney (HEK293T) cells were maintained in DMEM: F-12 medium, supplemented with 10% heat-inactivated FCS and 2 mM L-glutamine. HEK293T cells were grown to 80–90% confluence in six-well plates and transiently transfected with 1 µg plasmid encoding the human P2X receptor desired (hP2X1, hP2X2, hP2X3, hP2X4, hP2X5 or hP2X7) and 0.1 µg plasmid encoding the green fluorescent protein, using Lipofectamine 2000 (Invitrogen) as described previously (12). These plasmids are generous gifts from Prof. Alan R.North (University of Manchester, UK). The cells were then plated into Petri dishes and used for electrophysiological studies 24–72 h after transfection. All cells were grown at 37°C in a humidified 5% CO_2 incubator.

Reverse transcription–PCR analyses

Reverse transcription–PCR experiments were done using standard protocols in order to examine messenger RNA (mRNA) expression of P2Y and P2X receptors in cancer and non-cancer human cell lines. Total RNA extractions from cells were performed using NucleoSpin® RNA II (Macherey-Nagel, HOERDT, France), followed by reverse transcription using SUPERSCRIPT™ III (Invitrogen, UK) RNAse H-reverse transcriptase with oligo-deoxythymidine. Specific primers for human P2X and P2Y receptors, which were described in our recent study (29), were used in PCR. The temperature profile for PCR was 4 min at 94°C followed by amplification for 40 cycles, which consisted of 1 min at 94°C, 30 s at 60°C and 1 min at 72°C, and a final extension for 2 min at 72°C. PCR products were then analyzed by electrophoresis in 1.8% agarose gels containing ethidium bromide and visualized by ultraviolet trans-illumination.

Small interfering RNA transfection and efficacy assessment

MDA-MB-435s human breast cancer cells were transfected with 20 nM P2X7-small interfering RNA (siRNA) or scrambled siRNA, which were purchased from Tebu-Bio (Le Perray-en-Yvelines, France) as described previously (29), using Lipofectamine RNAi max (Invitrogen, France) according to the manufacturer's instructions and used 24 h after transfection. The efficiency of reducing the P2X7R expression by siRNA transfection was verified by quantitative PCR using an iCycler® system (Bio-Rad, Hercules, CA) as described previously (35). In brief, total RNA was extracted using NucleoSpin® RNA II (Macherey-Nagel), followed by reverse transcription using Ready-To-Go You-Prime First-Strand Beads, GE Healthcare (Fisher Scientific, Illkirch, France) RNAse H-reverse transcriptase and oligo-deoxythymidine. The following primers specific to the human P2X7R were used (forward primer: 5′-AAAACAGAAGGCCAAGAGCA-3′, reverse primer: 5′-CACCAGGCAGAGACTTCACA-3′). The PCR protocol consisted of a denaturation step at 95°C for 2 min, followed by 40 cycles of amplification at 95°C for 15 s, 60°C for 30 s and 72°C for 10 s. The efficiency of primers was >95% and a single product was seen on the melt curve analysis. Experiments were performed in triplicate and instead of water, the first-strand complementary DNA was used as negative control. Results were analyzed using the ΔC_t method, where the parameter C_t (threshold cycle) is defined as the cycle number at which the PCR reporter signal passes a fixed threshold. For each sample, the ΔC_t value was determined by subtracting the average C_t value of the investigated transcript in the cells transfected with scrambled siRNA from the average Ct value of the same transcript in the cells transfected with P2X7-siRNA. Transfections with siP2X7 reduced the P2X7R mRNA level by 65–90%.

Electrophysiological recordings

Patch clamp current recordings were made in the whole-cell configuration, using an Axopatch 200B patch clamp amplifier and a 1322A Digidata converter (Axon Instrument, CA), as described previously (11). The patch pipettes were prepared from borosilicate glass capillaries (WPI, Hertfordshire, UK) with a resistance of 4–6 MΩ. The cell capacitance and series resistances were electronically compensated. The membrane potential was held at −60 mV. Experiments were performed at room temperature (20–25°C) in a standard external physiological saline solution (PSS) and pipettes were filled with an intracellular solution (see Solutions). ATP was externally applied to the patched cells for 5 s when examining the P2X1, P2X2 and P2X3 receptors and for 10 s when examining P2X4, P2X5 and P2X7Rs, at the indicated concentrations, using a RSC-160 fast-flow delivery system (BioLogic Science Instruments, Claix, France). When studying the P2X7R, emodin was perfused onto the patched cells at the indicated concentrations for 4 min before ATP was applied again to induce the currents. The emodin concentration–response relationship was analyzed by least squares fitting of the mean data to the following modified Hill equation: $y = (A_1 - A_2)/(1 + (x/x_0)^p) + A_2$, where A_1 and A_2 represent the ATP-induced currents in the absence or the maximal concentrations of emodin, respectively, x_0 is the concentration reducing the emodin-sensitive currents by 50%, and p is the Hill coefficient. The concentration–responses curve was plotted using Origin Microcal 6.0 software (Microcal Software, Northampton, MA). When studying the other P2X receptors, emodin was perfused onto the patch cells at the maximal 10 µM concentration. Because all P2X receptors, except P2X7R, show a current desensitization, we performed multiple applications of 10 µM ATP (from 2 to 5, depending on the receptor). ATP applications were performed every 4 min in presence or not of emodin (10 µM). The potential effect of emodin was analyzed on the desensitization curves built by measuring the maximal current (I) triggered for each ATP application divided by the maximal current (I_{max}) recorded at the first application. The desensitization curve was fitted by the following monoexponential decay equation: $y = A \exp(-x/t) + y_0$.

Solutions

The external PSS had the following composition (in millimolar): 147 NaCl, 10 *N*-2-hydroxyethylpiperazine-*N*′-2 ethanesulfonic acid, 13 D-glucose, 2 KCl, 2 $CaCl_2$ and 1 $MgCl_2$. The intracellular solution for the patch clamp recording experiments had the following composition (in millimolar): 147 NaCl, 2 KCl, 10 *N*-2-hydroxyethylpiperazine-*N*′-2 ethanesulfonic acid and 10 ethyleneglycol-bis-(2-aminoethylether)-*N*,*N*,*N*′,*N*′-tetraacetic acid. The osmolarity and pH values for both solutions were 295–315 mOsm and 7.3, respectively. Emodin was prepared as 10 mM stock solution in dimethyl sulfoxide (DMSO) as the vehicle solvent. The working solutions of ATP and emodin were prepared in PSS (for the patch clamp recordings and Ca^{2+} measurements) and in normal culture medium DMEM supplemented with 5% FCS (for the cell viability, DQ-gelatin and invasiveness experiments) at the indicated concentrations. All the solutions for the control experiments contained the matched volume of DMSO.

Western blotting

Western blotting of cell lysates was performed according to standard protocols to examine the P2X7R protein expression in MDA-MB-435s and MCF-10A cells. In brief, cell lysates were prepared by washing the cells twice in phosphate-buffered saline (PBS), and then lysing them in RIPA buffer (20 mM Tris–HCl pH 7.4, 150 mM NaCl, 1 mM $MgCl_2$, 1 mM $CaCl_2$) with 1% Triton X-100 and supplemented with complete protease inhibitor cocktail (Sigma–Aldrich) for 1 h at 4°C. The cell lysates were cleared by centrifugation at 16 000*g* for 10 min. Total protein concentrations were determined using the Pierce® BCA Protein Assay Kit Thermo scientific (Fisher Scientific). Protein sample buffer was added and the samples were boiled at 100°C for 3 min. Total protein samples (60 µg) were electrophoretically separated by sodium dodecyl sulfate–polyacrylamide gel electrophoresis in 10% gels, and then transferred to polyvinylidene difluoride membranes (Millipore, Molsheim, France). The P2X7R proteins were detected using primary polyclonal rabbit anti-P2X7 primary antibody at a dilution of 1:200 (Alomone Labs, Jerusalem, Israel) and secondary horseradish peroxidase-conjugated goat antirabbit IgG secondary antibody at 1:2000 (Tebu-Bio). The HSC70 proteins used for sample loading control were detected using primary mouse anti-HSC70 at 1:30 000 (TebuBio) and secondary horseradish peroxidase-conjugated

antimouse-IgG antibodies at 1:2000 (Tebu-Bio). Proteins were visualized using a Electrochemiluminescence-Plus Kit (Pierce® ECL Western Blotting Substrate; Fisher Scientific) and captured on Kodak Bio-Mark MS films (Sigma–Aldrich, France).

Measurement of intracellular Ca^{2+} concentrations

Changes in internal free calcium concentration were monitored by the fluorescent ratiometry using Fura-2/AM Ca^{2+} indicator. MDA-MB-435s cells were seeded 1×10^6 cells per well in six-well plates 48 h before use. After washing in PBS, the cells were incubated in the Optimem media (GIBCO, Invitrogen, Saint Aubin, France) containing 2.5 µM Fura-2/AM (Invitrogen, France) at 37°C for 50 min. The cells were washed gently with PBS and then scraped in 10 ml Optimem media. After 5 min centrifugation at 700*g* at room temperature, the supernatant was discarded and the cells were resuspended in 2 ml PSS (see Solutions). The cell suspension was loaded into the cuvette of the spectrofluorimeter (Hitachi F-2500, Courtaboeuf, France, Japan) and was kept under agitation at room temperature. Fluorescence was alternatively excited by 340 and 380 nm and measured at 510 nm, and the F340/F380 ratio was calculated. A438079 and emodin were added to the cell suspension 5 min before stimulation with 3 mM ATP. In the end of each experiment, 2.5 µM ionomycin (Sigma–Aldrich) was added in order to induce the maximal Ca^{2+} loading of the cell preparations. ATP-induced changes in the F340/F380 ratio were expressed as percentage of those induced by ionomycin in the same cell preparations.

Cell viability assay

To assess the cell survival, cancer or non-cancer cells were seeded at 1.5×10^4 cells per well in 24-well plates in their respective culture medium (see Measurement of intracellular Ca^{2+} concentrations) that contained different concentrations of emodin (from 1 nM to 10 µM) or the matched volume of DMSO used as a vehicle for emodin. The cells were grown for 4 days and the media were replaced daily. The living cell numbers were determined using the tetrazolium salt assay as described previously (35). The cell viability was expressed as formazan absorbance at 570 nm and expressed as a percentage of the control condition in the absence of emodin. Results were validated by manual cell counting. Three independent experiments were performed.

Cell invasiveness assays and cell morphology analyses

The cell invasiveness was analyzed in 24-well plates receiving 8 µm pore size polyethylene terephthalate membrane cell culture inserts covered with a film of Matrigel® (BD Biosciences, France). The upper compartment was seeded with 4×10^4 cells in the basal culture medium. The lower compartment was filled with the culture medium supplemented with 10% FCS, instead of 5%, as a chemoattractant. After 24 h of incubation at 37°C, the cells attached to the side of the inserts facing the lower compartment were stained with hematoxylin and counted under a light microscope. The cell invasiveness assays were performed in triplicates in 3–8 separate experiments. For meaningful comparison between separate experiments, the cell numbers were normalized to that under the control condition (vehicle) in the absence of drug or ATP.

The change in cell morphology was assessed from images of hematoxylin-stained MDA-MB-435s using the ImageJ© software 1.38I (http://rsbweb.nih.gov/ij). A circularity index was calculated as being $4\pi \times (\text{area})/(\text{perimeter})^2$. As the value approaches 0, it indicates an increasingly elongated shape and, conversely, the value of 1.0 indicates a perfect circle.

Assessment of gelatinolytic activity of cancer cells

MDA-MB-435s cells were cultured in a 3D-Matrigel® matrix containing 25 µg/ml DQ-Gelatin® (Invitrogen, France) on glass coverslips for 24 h and then fixed in 4% paraformaldehyde in PBS at room temperature for 10 min as described previously (36). Epifluorescence microscopy was performed with a Nikon TI-S (Champigny sur Marne, France). The samples were excited at 495 nm and the emission at 515 nm was recorded. The fluorescence density was quantified using the ImageJ© software 1.38I.

*Zebrafish maintenance and **in vivo** zebrafish metastatic assays*

Zebrafish (ZF; *Danio rerio*), from the Zebrafish International Resource Centre, were maintained in re-circulating tanks according to standard procedures (*The zebrafish handbook: a laboratory use of zebrafish, Brachydanio rerio*). Adult fish were maintained at 26°C, with a light/dark cycle of 14/10 h and were fed twice daily, once with dry flake food (PRODAC) and once with live arthemia (MC 450, IVE AQUACULTURE). ZF embryos were maintained in egg water at 28.5°C and were fed for 5 days with NOVO TOM and with live arthemia at 11 days of life. The experiments were performed in compliance with the Guidelines of the European Union Council for animal experimentation (86/609/EU) and were approved by the bioethical committee of the University Hospital Virgen de la Arrixaca (Spain). The development of micrometastases in ZF embryos was described previously (29). Briefly, MDA-MB-435s or MDA-MB-468 breast cancer cells were trypsinized, washed and stained with the vital cell tracker red fluorescent CM-Dil (Vibrant; Invitrogen). Labeled cells were pre-incubated for 30 min with 1 or 10 µM emodin or vehicle (DMSO), and 50 labeled cells were injected into the yolk sac of dechorionated ZF embryos using a manual injector (Narishige, London, UK). Fish with fluorescently labeled cells appearing outside the implantation area at 2 h were excluded from further analysis. All other fish were incubated at 35°C for 48 h and analyzed with a SteReo Lumar V12 stereomicroscope with an AxioCam MR5 camera (Carl Zeiss, Barcelona, spain). The evaluation criteria for micrometastases were the presence of more than five cells outside of the yolk. Injection of emodin or vehicle into the yolk sac of ZF embryos did not affect the development of the fish and did not affect the viability of cancer cells. A ZF metastasis index was calculated as being the proportion of embryos showing micrometastases in each condition divided the proportion of embryos showing micrometastases in the control condition in absence of emodin.

Data analysis and statistics

The average results are expressed as mean ± standard error of the mean from the number of cells or essays indicated in the figure legends. Statistical analyses were performed using SigmaStat 3.0.1a (Systat Software, Chicago, IL) using Student's *t*-test, or alternatively Mann–Whitney rank sum test when the variance homogeneity test failed. Statistical significance is indicated as follows: $*P < 0.05$; $**P < 0.01$ and $***P < 0.001$.

Chemicals, salts and drugs

General chemicals, ATP, emodin and 3-(4,5-dimethylthiazol-2-yl)-3,5-diphenyltertrazolium bromide were obtained from Sigma–Aldrich (France). Flura-2/AM was purchased from Invitrogen (France), and A438079 was obtained from Tocris (Lille, France).

Results

We first examined the mRNA expression of P2X receptors in several human cell lines: MCF-10A non-cancer mammary cells, MDA-MB-468 and MDA-MB-435s, which represent weakly and highly invasive breast cancer cells, respectively, and A549 non-small cell invasive lung cancer cells. Although MCF-10A and MDA-MB-468 cells did not express or weakly expressed P2X7R, A549 and MDA-MB-435s cells expressed a much higher level of mRNA for P2X7R (Figure 1A). There was detectable mRNA expression for P2X4, P2X5 and P2X6 (Figure 1A) but the expression level was correlated with cell invasiveness, in contrast with the expression of mRNA for P2X7R. The mRNA expression profile for P2Y receptors was also studied and showed that all cell types express multiple P2Y receptors with the exception of MDA-MB-435s cells only expressing mRNA for P2Y11 receptors (Figure 1B). Therefore, it is the expression of the P2X7R in cancer cells that could be associated with a high invasive capacity. Western blotting experiments further showed expression of P2X7 proteins in highly invasive human cancer cells, MDA-MB-435s (breast) and A549 (lung), and not in the non-cancer MCF-10A cells or the weakly invasive MDA-MB-468 cells (Figure 1C).

We then tested the effect of emodin (Figure 2A) on the cell viability of MDA-MB-435s and A549 human cancer cells. The cells were treated for 4 days with increasing doses of emodin from 1 nM to 10 µM. Emodin at a concentration of ≤1 µM had no discernible effect on, and at 10 µM caused a very mild but significant reduction in, the cell viability (Figure 2B). We repeated such experiments on MCF-10A non-cancerous mammary and MDA-MB-468 breast cancer cells, which unlike MDA-MB-435s and A549 cells do not express the P2X7Rs (Figure 1A and C). Virtually, the same results were observed (Figure 2B). These results, therefore, indicate that emodin for concentrations of 1 µM or less is neither toxic nor antiproliferative for the human mammary cells tested.

We have recently shown that the P2X7Rs are a key determinant in promoting the invasive phenotype of the highly aggressive MDA-MB-435s human cancer cells, through the release of active cathepsins in the extracellular microenvironment (29). In a separate study, we have shown emodin as a potent antagonist at the rat P2X7Rs endogenously expressed in peritoneal macrophages or heterologously expressed in HEK293T cells (34). To test the potential antagonism of emodin on the human P2X7R, we examined the effect of emodin on the human

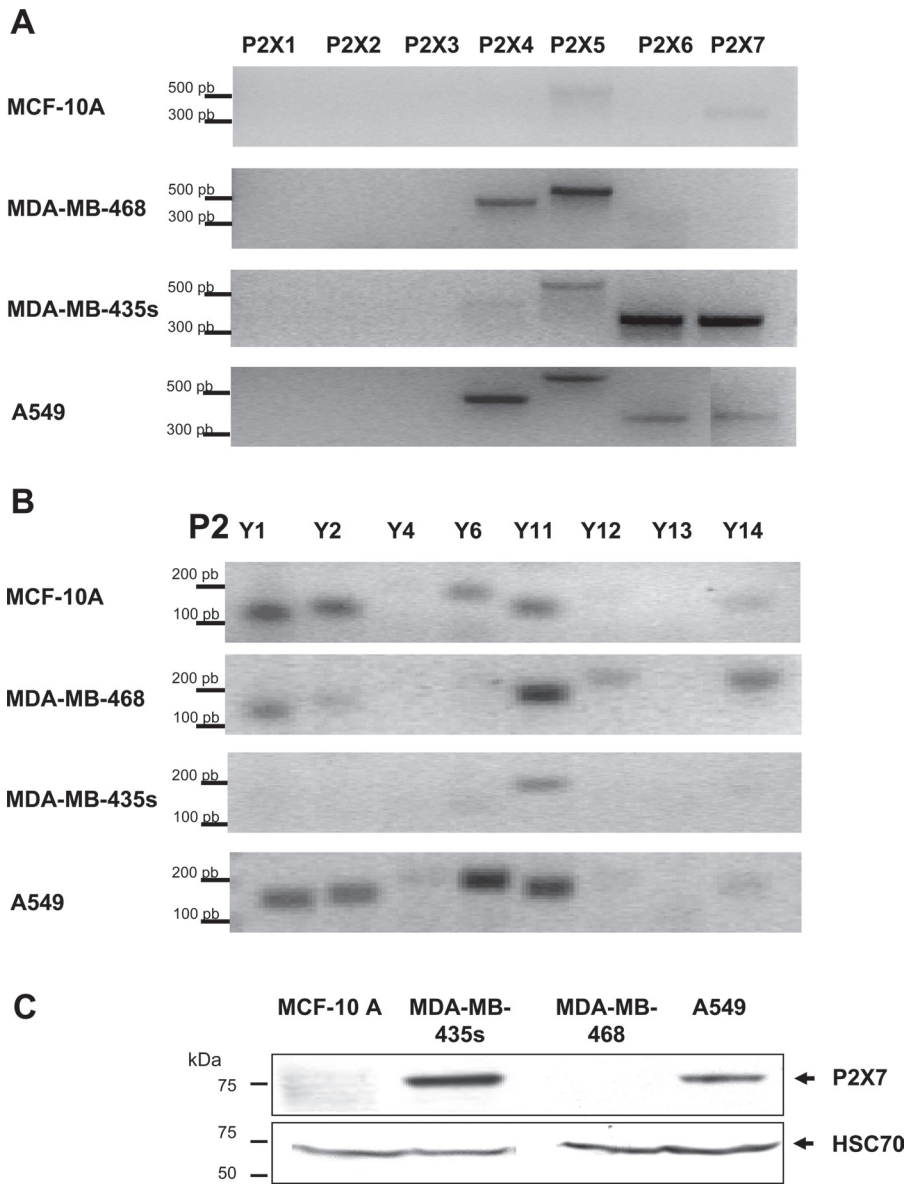

Fig. 1. Expression profile of P2 receptors in human non-cancer and cancer cell lines. (**A** and **B**) Representative reverse transcription–PCR experiments analyzing the expression of mRNA for the P2X (A) and P2Y receptors (B) in human non-cancerous mammary MCF-10A cells, weakly invasive MDA-MB-468 cells, highly invasive (MDA-MB-435s) human breast cancer cells and A549 human non-small cell lung cancer cells. (**C**) Representative western blotting experiments showing protein expression of the P2X7R in MDA-MB-435s breast and A549 lung cancer cells but not in MCF-10A non-cancerous mammary and MDA-MB-468 breast cancer cells. HSC70 was used as a control for sample loading.

P2X7R-dependent increase in the intracellular Ca^{2+} concentration $[Ca^{2+}]_i$ in MDA-MB-435s cancer cells and human P2X7R-mediated currents in HEK293T cells (Figures 2 and 3). As shown on Figure 2C and E, 3 mM ATP induced a sustained increase in the $[Ca^{2+}]_i$ in MDA-MB-435s cells, which was completely abolished when the cells were pre-incubated with 10 µM A438079, a P2X7R-selective antagonist (37), suggesting that P2X7R is the predominant P2X receptor-mediating ATP-induced increase in the $[Ca^{2+}]_i$ in MDA-MB-435s cancer cells (29). Such ATP-induced increase in the $[Ca^{2+}]_i$ was dose dependently inhibited by pre-incubation with emodin (1 and 10 µM; Figure 2D and E). Emodin on its own had no effect on the $[Ca^{2+}]_i$ when compared with its vehicle (data not shown). We also examined the effect of emodin on ATP-evoked currents, using whole-cell patch clamp recordings in HEK293T cells heterologously expressing the human P2X7R and compared this to the effect on other human P2X receptors (Figure 3). Treatment with 10 µM emodin for 4 min solely inhibited ATP-evoked currents recorded in the P2X7R-expressing cells, whereas it had no effect on P2X1, P2X3, P2X4 and P2X5 receptors and slightly but significantly increased the ATP-mediated current triggered in P2X2R-transfected cells (Figure 3A and B). Accumulative treatment of the patched cells with emodin for 4 min inhibited ATP-evoked P2X7-dependent currents in a concentration-dependent manner, with a maximal inhibition of approximately 70% (Figure 3C). The concentration–response curve was well fitted by the Hill equation. The ATP-induced currents were inhibited by 50% at about 3 µM. Because the P2X1–P2X5 receptors show current desensitization (10), we also checked for a specific effect of emodin on the desensitization of these receptors. We performed whole-cell patch clamp experiments in HEK293T expressing the human homomeric P2X1–P2X5 receptors, stimulating the cells with repetitive application of 10 µM ATP in presence or not (control) of 10 µM emodin allowing the fitting of desensitization curves (Supplementary Figure S1, available at *Carcinogenesis* Online). We found that emodin had no significant effect on these P2X receptors except that it slightly slowed down desensitization of the hP2X2 receptors. Taken together, these results indicate that emodin inhibits human P2X7R-mediated Ca^{2+}

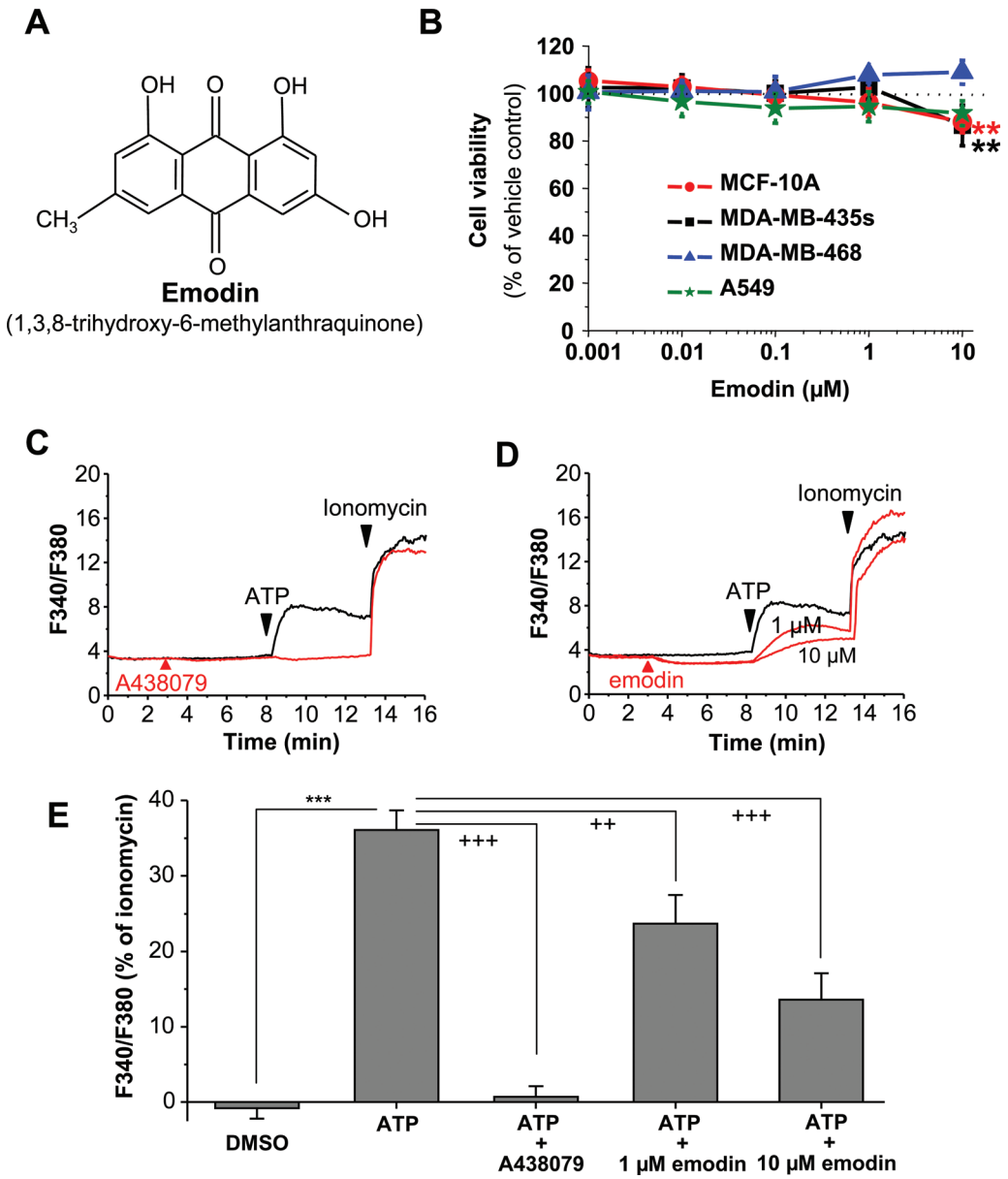

Fig. 2. Effects of emodin on cell viability and on the activity of human P2X7Rs in MDA-MB-435s human breast cancer cells. (**A**) Structure of emodin, an anthraquinone derivative isolated from *R.officinale* Baill. (**B**) Cell viability of MCF-10A human non-cancerous mammary (red circles), MDA-MB-468 (blue triangles), MDA-MB-435s human breast cancer (black squares) and A549 (green stars) human non-small cell lung cancer cells, after 4 days in cell culture with indicated concentrations of emodin, expressed as a percentage of the control condition (vehicle). These results are from three independent experiments. ** indicates a significant difference to the control condition at $P < 0.01$, using Mann–Whitney rank sum test. (**C**) Inhibition by emodin of ATP-induced P2X7R-mediated Ca^{2+} influx in MDA-MB-435s cancer cells. The panel shows representative changes in the intracellular Ca^{2+} concentrations $[Ca^{2+}]_i$ using Fura-2 to monitor changes in F340/F380 or the ratio of the emission fluorescence at 510 nm induced by excitation at wavelengths of 340 and 380 nm. The $[Ca^{2+}]_i$ were increased when the cells were stimulated with 3 mM ATP (ATP), which were prevented by pre-treatment with P2X7R antagonist (C) A438079 (10 μM) or (**D**) emodin (1 and 10 μM; right). Ionomycin (2.5 μM) was applied in the end of the experiments to show the maximal increase in the $[Ca^{2+}]_i$. (**E**) Histograms summarizing mean data from three independent experiments. The Fura-2 fluorescence or F340/F380 under the indicated test conditions was expressed as % of that induced by ionomycin. *** significant difference from the DMSO vehicle condition at $P < 0.001$; $^{++}$ and $^{+++}$, significant difference from the ATP condition at $P < 0.01$ and $P < 0.001$, using Student's *t*-test.

entry and currents, as shown previously for the P2X7R-mediated Ca^{2+} entry in rat macrophages and currents in HEK293 cells heterologously expressing the rat P2X7R (34).

An important feature for the development of metastases is the capacity of cancer cells to degrade the ECM, through the release or activation of numerous proteases such as matrix metalloproteinases (38) or cysteine cathepsins (39). Our recent study has shown that the P2X7R expression is strongly upregulated in MDA-MB-435s cancer cells and stimulation of the P2X7Rs with ATP remarkably promotes cell invasiveness through the release of active cysteine cathepsins (29). Therefore, we tested whether emodin as a P2X7R antagonist inhibited ATP-induced ECM proteolysis. MDA-MB-435s cancer cells were grown for 24 h in a three-dimensional matrix of Matrigel®, mimicking the ECM and containing DQ-gelatin, which releases fluorescent products after proteolytic cleavage by gelatinases. As shown on Figure 4A, the gelatinolytic activity was low and mainly distributed at the pericellular zone of the untreated cells. Stimulation of the cells with 3 mM ATP remarkably increased gelatinolysis of the pericellular matrix. Such ATP-induced effect was totally abolished in the presence of 1 μM emodin (Figure 4B).

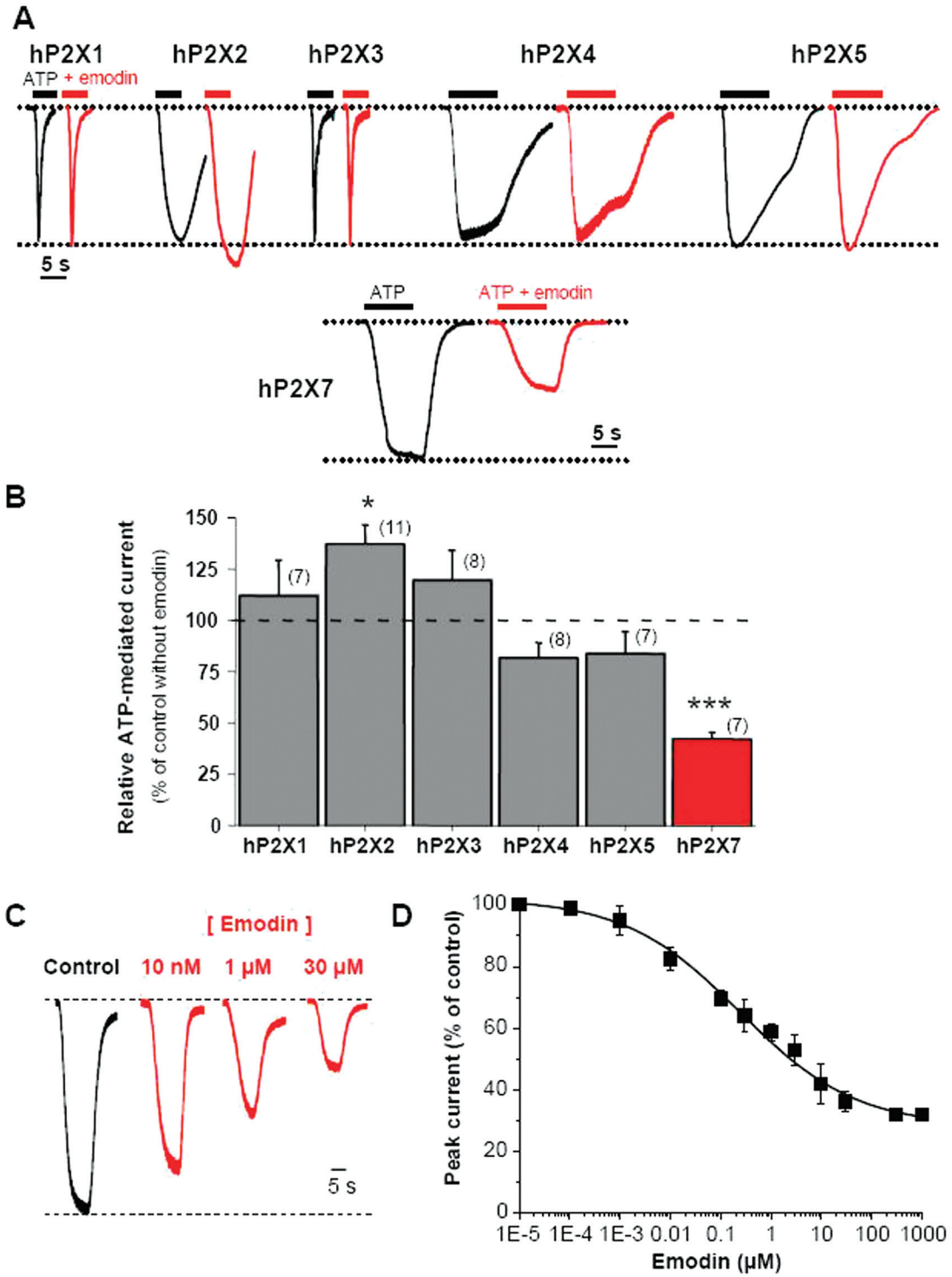

Fig. 3. Emodin inhibits ATP-induced P2X7R currents. (**A**) Representative traces showing whole-cell ATP-induced currents recorded from HEK293T cells transiently transfected with human P2X1, P2X2, P2X3, P2X4, P2X5 or P2X7Rs, at a holding potential of −60 mV in the absence (control, black traces) or after 4 min pre-treatment with 10 µM emodin (red traces). In the case of fast-desensitizing P2X1, P2X2 and P2X3 receptors, ATP was applied for 5 s at a concentration of 10 µM. For studying P2X4 and P2X5 receptors, ATP was applied for 10 s at a concentration of 10 µM. P2X7Rs were stimulated by 3 mM ATP for 10 s. (**B**) Relative summary of the mean effect of 10 µM emodin on the ATP-induced inward currents mediated by different human P2X receptors heterologously expressed in HEK293T cells. Numbers in brackets represent the number of studied cells for each receptor. * indicates a significant difference at $P < 0.05$, and *** at $P < 0.001$, compared with the control current without emodin. (**C**) Inhibition by emodin of ATP-induced currents in HEK293T cells transiently transfected with human P2X7R. At the left are representative whole-cell current recordings at a holding potential of −60 mV and in response to 10 s application of 3 mM ATP in the absence (control) and the presence of increasing concentrations of emodin are shown. At the right, the mean data are summarized ($n = 2$–7 for each data point). The emodin concentration–inhibition curve was derived by fitting the mean data to the Hill equation indicating an IC_{50} of approximately 3 µM.

We went on to assess the ability of emodin to reduce P2X7-positive MDA-MB-435s cancer cells invasiveness *in vitro* and *in vivo*. We studied the *in vitro* invasive properties of MDA-MB-435s cancer cells in relationships with the P2X7R stimulation, using the invasion inserts with the filters coated with Matrigel™, which mimics the ECM. As shown in Figure 5A, it is clear that ATP strongly increased the cell invasion,

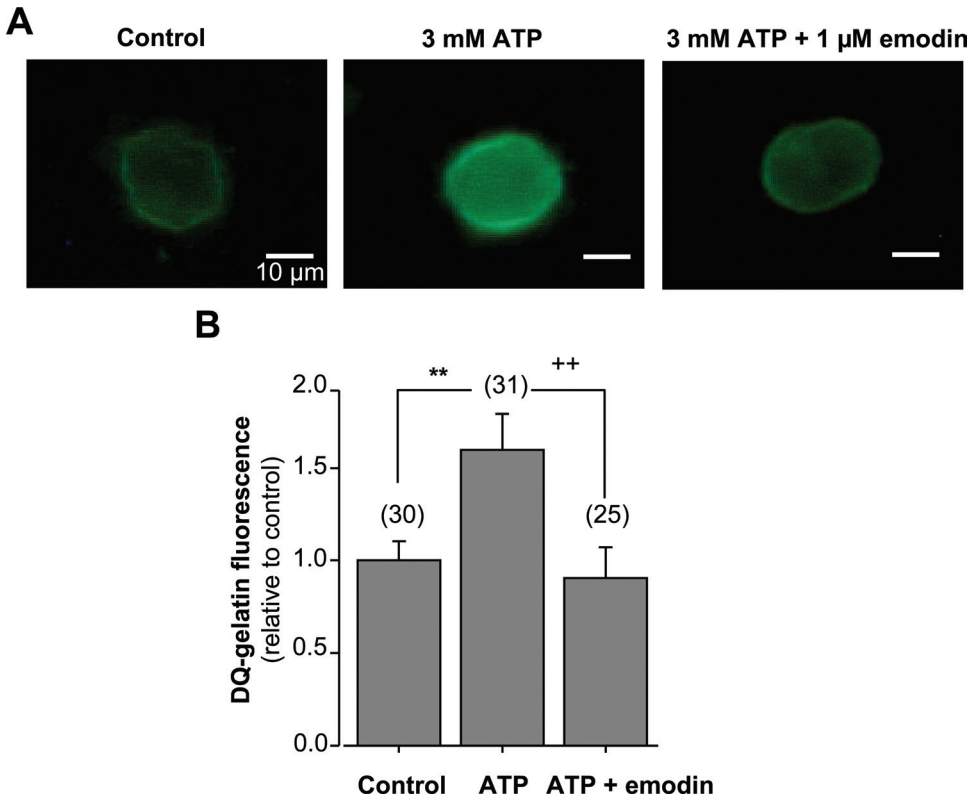

Fig. 4. Inhibition by emodin of ATP-induced gelatinolytic activity of MDA-MB-435s breast cancer cells. (**A**) Representative fluorescence images of MDA-MB-435s cancer cells grown for 24 h within a 3D-Matrigel® matrix containing DQ-Gelatin® (as a fluorogenic substrate for gelatinases) for the vehicle control, 3 mM ATP and 3 mM ATP in the presence of 1 µM emodin. (**B**) The diagram summarizes the fluorescence intensity relative to the control condition (n = 25–31). ** indicates a significant difference at $P < 0.01$ compared with the control condition, and $^{++}$ indicates a significant difference at $P < 0.01$ compared with the ATP condition.

and such ATP-induced effect was completely prevented in the presence of 1 µM emodin. These effects were not altered in the MDA-MB-435s cancer cells transfected with scrambled siRNA (siCTL); stimulation with 3 mM ATP massively increased the cell invasion by 2.2 ± 0.3 times, which was abolished by emodin. In the cells transfected with P2X7-siRNA, the basal cancer cell invasiveness in the absence of ATP stimulation was reduced by 56% (Figure 5B). Furthermore, silencing the P2X7R expression led to complete loss of both the increase in cell invasion induced by ATP and the inhibition by emodin (Figure 5B). The efficacy of cell transfection with siP2X7 as compared with siCTL was assessed by reverse transcription–quantitative PCR, as indicated in the Materials and methods, and reduced the P2X7R mRNA level by 65–90%. ATP also induced substantial changes in the cell morphology of the wild-type and scrambled siRNA-transfected MDA-MB-435s cancer cells, resulting in 'neurite-like' cell elongation (Figure 5A), which is the hallmark of increased invasive abilities. In order to quantify such changes in the cell morphology, we calculated the circularity index (see Materials and methods) from the cells transfected with scrambled siRNA or P2X7-siRNA. The value of approaching to 0 indicates that the cell has an increasingly elongated shape and, conversely, the value of 1.0 denotes a perfect circle. For the scrambled siRNA-transfected cells, the circularity index was 0.61 ± 0.02 (n = 77 cells) for the non-stimulated cells, and the circularity index significantly decreased to 0.49 ± 0.01 (n = 305 cells) for the cells stimulated with 3 mM ATP and 0.62 ± 0.02 (n = 104 cells) for the cells stimulated with 3 mM ATP in the presence of 1 µM emodin (Figure 6C). Such ATP-induced decrease in the circularity index and inhibition by emodin were not observed in the cells transfected with P2X7-siRNA (Figure 5C). Comparative experiments were performed for P2X7-negative MDA-MB-468 cancer cells showing that ATP (3 mM) alone, or in presence of emodin (10 µM) or A438079 (10 µM), had no effect on cell invasiveness (Figure 5D) or on cell morphology (Figure 5E). The invasion capacity of P2X7-positive A549 non-small cell cancer cells was also analyzed (Supplementary Figure S2, available at *Carcinogenesis* Online). Stimulating these cells with 3 mM ATP induced a 4-fold increase in matrix invasion, which was prevented by the use of emodin (10 µM) or the P2X7 antagonist A438079 (10 µM). Taken together, these results strongly indicate that the P2X7Rs are critically involved in determining the cancer cell invasiveness *in vitro* and the inhibitory action of emodin results from antagonisms of the P2X7Rs.

We finally analyzed the effect of emodin on the MDA-MB-435s cancer cell invasion *in vivo* using the ZF model of micrometastasis (40), which has been used in our recent study to demonstrate the involvement of P2X7R in promoting *in vivo* invasiveness (29). Approximately, 35% of the ZF embryos injected with MDA-MB-435s cells presented more than five cells outside of the yolk sac 48 h after injection, but only 21 and 19% of the embryos presented micrometastases when the MDA-MB-435s cells were treated with 1 and 10 µM emodin, respectively (Figure 6B), resulting in a decrease of the ZF micrometastasis index of 41 ± 10% and 47 ± 8%, respectively. This indicated that emodin can suppress the micrometastases or *in vivo* invasion of MDA-MB-435s cells. Comparative studies were performed with the injection of P2X7-negative MDA-MB-468 cancer cells and showed that emodin (10 µM) did not reduce the ZF micrometastasis index.

Discussion

The development of metastases importantly relies on, at the cellular level, the ability of cancer cells to degrade, and migrate through, the ECM. P2X7R is an intriguing receptor first characterized as a cytolytic receptor (P2Z) because its sustained activation generally leads to cell death (13,14). It is also responsible for important physiological responses such as triggering the inflammatory signaling cascade after

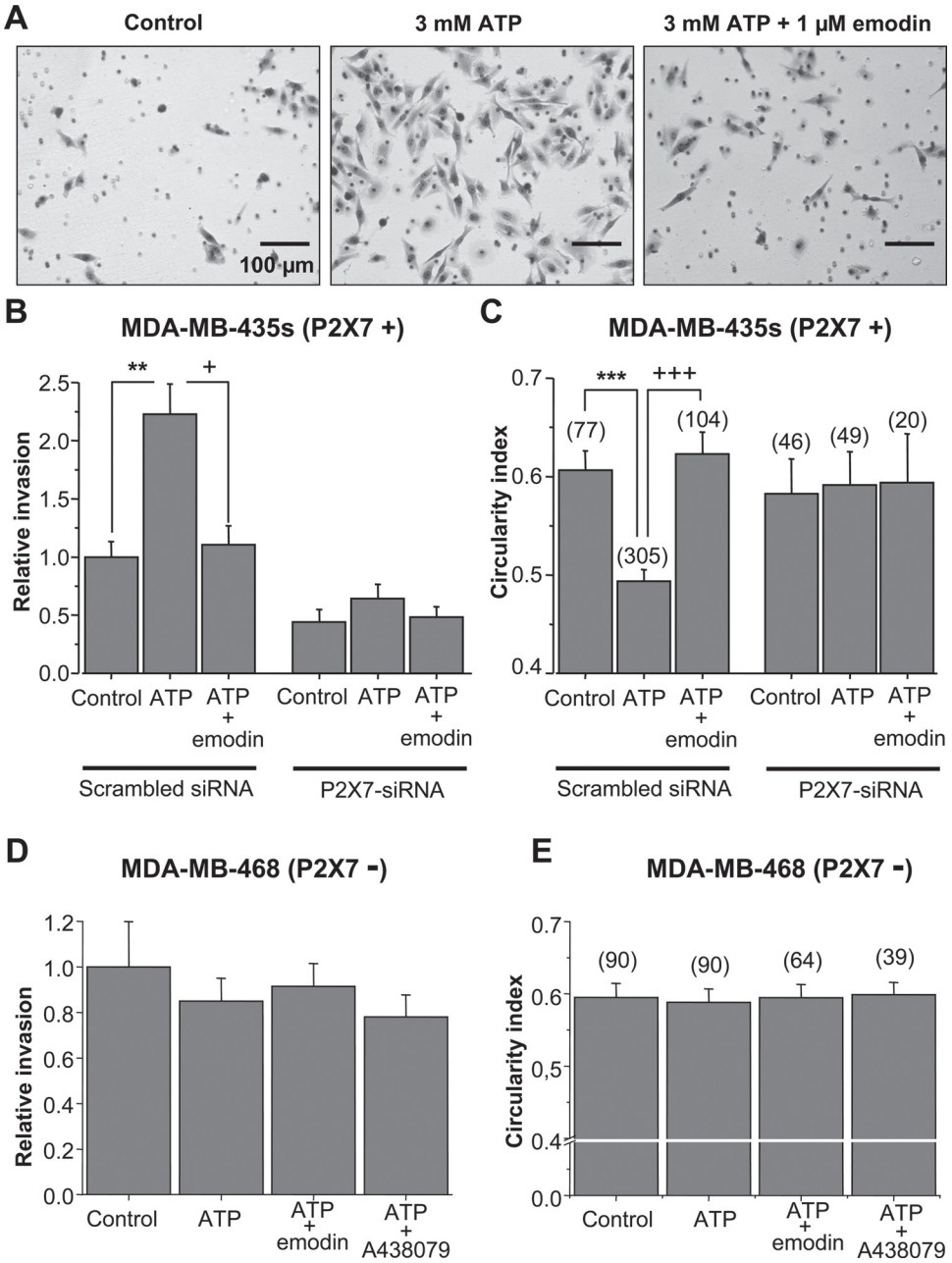

Fig. 5. Inhibition by emodin of P2X7R-induced *in vitro* pro-invasive phenotype of MDA-MB-435s breast cancer cells. (**A**) Shown are representative images of fixed and hematoxylin-stained MDA-MB-435s (P2X7+) cell invasion on the Matrigel®-coated inserts in the presence of vehicle (control), 3 mM ATP or 3 mM ATP and 1 µM emodin. The MDA-MB-435s cells were transfected with scrambled siRNA. (**B**) The summary of the invasion results from eight independent experiments, as the one shown in A, for the MDA-MB-435s cells were transfected with scrambled siRNA or siRNA directed against the expression of the *P2RX7* gene (P2X7-siRNA). The results were expressed relative to the control cells transfected with scrambled siRNA. ** denotes a significant difference from the control at $P < 0.01$, and $^{+}$ a significant difference from the ATP condition at $P < 0.05$, using Mann–Whitney rank sum test. (**C**) The summary of the circularity index from eight independent experiments, as the one shown in A, for the MDA-MB-435s cells were transfected with scrambled siRNA or P2X7-siRNA. The numbers in bracket indicate the number of cells examined in each case. (**D**) The invasion of MDA-MB-468 breast cancer cells, not expressing P2X7Rs (P2X7−), was also studied in control condition (vehicle), or under stimulation with 3 mM ATP alone or in presence of emodin (10 µM) or A438079 (10 µM; three independent experiments). (**E**) The summary of the circularity index of MDA-MB-468 cells calculated from experiments and conditions indicated in D was studied. The numbers in bracket indicate the number of cells examined in each case. *** denotes a significant difference from the control at $P < 0.001$, and $^{+++}$ denotes a significant difference from the ATP condition at $P < 0.001$, using Mann–Whitney rank sum test.

tissue damage or infection (15). Recent studies have shown the P2X7Rs to be expressed at much higher or increased levels in several tumors compared with normal tissues (5,19–25). The only exception, to our knowledge, is the cervical cancer cells in which the P2X7R expression is downregulated (41). Furthermore, some of these studies have reported the P2X7R to exhibit pro-cancerous properties, albeit in different ways depending on the cancer types: imposing antiapoptotic effects (24) or sustaining cell growth (5,27,42). Our recent study has provided evidence to support that activation of the P2X7Rs promotes cancer cell invasiveness (29). These findings are in line with other studies of thyroid carcinoma (43) and lymphoid neoplasm (44) and taken together support an important role for the P2X7Rs in the development of metastases. This has led to the hypothesis that selective antagonism of the P2X7Rs may represent a new strategy for cancer therapeutics (8).

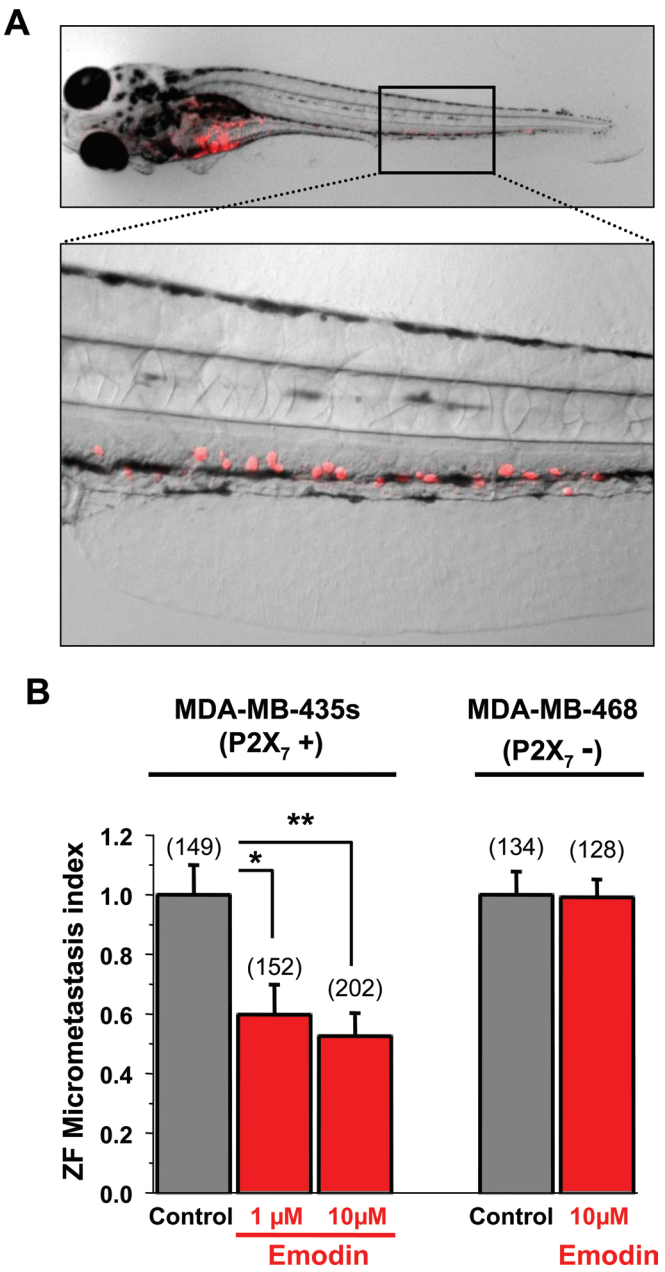

Fig. 6. Inhibition by emodin of the *in vivo* invasiveness of P2X7-positive MDA-MB-435s and not of P2X7-negative MDA-MB-468 breast cancer cells. (**A**) Representative image of a ZF embryo injected with MDA-MB-435s cells and showing micrometastases. A magnification of the highlighted region of the embryo with metastasis is shown below. (**B**) Mean ZF micrometastasis index of P2X7-positive MDA-MB-435s cancer cells in the presence of the vehicle (control), or 1 or 10 µM emodin, and of P2X7-negative MDA-MB-468 cancer cells in the presence of the vehicle (control), or 10 µM emodin. The numbers in bracket indicate the number of embryos examined for each condition from three different experiments. * and ** indicate significant differences from the control condition at $P < 0.05$ and $P < 0.01$, respectively, using Student's *t*-test.

Emodin is an anthraquinone-derived compound. This and structurally related compounds have been demonstrated to possess antitumor properties as well as immune-suppressive abilities (30,31). Our recent study has demonstrated that emodin acts as a potent P2X7R antagonist, inhibiting rat P2X7R-mediated Ca^{2+} influx in peritoneal macrophages and also reducing BzATP-induced currents in HEK293 cells heterologously expressing the rat P2X7R (34). Consistently, we showed in this study that emodin strongly inhibited the human P2X7R and ATP-induced Ca^{2+} influx in MDA-MB-435s cells without strong effect on the cell viability (Figure 2B–E). Emodin at 1 µM strongly or completely inhibited ATP-induced ECM proteolysis in these human breast cancer cells (Figure 4). Moreover, emodin prevented ATP-induced increases in the P2X7-positive breast (Figure 5B) and lung (Supplementary Figure S2, available at *Carcinogenesis* Online) cancer cell invasiveness *in vitro* and the associated changes in cell morphology (Figure 5C), whereas it had no effect on P2X7-negative MDA-MB-468 cancer cells (Figure 5D and E). Such inhibitory actions by emodin as well as the ATP-induced effects were completely abolished by silencing the P2X7R expression (Figure 5B–C). Finally, emodin strongly inhibited the P2XR-dependent cancer cell invasion *in vivo* (Figure 6). Therefore, this study has provided several lines of consistent evidence to show that emodin suppresses the human cancer cell invasiveness by antagonizing the P2X7R.

Reactive blue 2 and Cibacron blue are anthraquinone–sulfonic acid derivatives and are known to be effective as non-selective and non-competitive P2 receptor antagonist (45). Anthroquinone–sulfonic acids are also known to act on many of the enzymes concerned with purine metabolism (46). Alkyl- and aryl-amino-substituted anthraquinone derivatives have also been synthesized recently and one of them was shown to be a potential P2Y12 platelet receptor antagonist (47). We cannot exclude the possibility that emodin could modulate the activity of some P2Y receptors, and especially P2Y12 receptors that can be modulated by anthraquinone derivatives (47). However, the P2Y12 receptors are not expressed in MDA-MB-435s cells (Figure 1B). In addition, in cells expressing P2Y12 receptors but not P2X7Rs, such as in MDA-MB-468 cells, ATP and emodin, used alone or in combination, had no effect on cell viability or cell migration. Thus, the inhibition by emodin on ATP-induced invasive effects described in this study is highly unlikely to be mediated by the P2Y12 receptor. In this study, emodin has been found to specifically inhibit P2X7Rs functioning and not the other human P2X receptors expressed as homomers in HEK293T. No inhibitory effect was found in the closely related human P2X4 receptor, as reported for the rat P2X4 receptor by our previous study (34). Only a mild effect was found on the hP2X2 receptor at which emodin, at a maximal concentration of 10 µM, reduced the receptor desensitization.

The discovery of emodin as a potent P2X7 antagonist with a potent inhibitory action on the human breast and lung cancer invasiveness substantiates the concept that the P2X7Rs is a promising therapeutic target and suggests emodin as a starting compound for development of lead compounds and ultimately new therapeutic drugs to be used for prevention and treatment of metastatic breast, lung and other cancers.

In conclusion, we have shown that emodin, a compound with known antitumor property, suppresses human breast cancer cell invasiveness *in vitro* and *in vivo* by antagonizing the P2X7Rs.

Supplementary material

Supplementary Figures 1 and 2 can be found at http://carcin.oxfordjournals.org/

Funding

Ligue Nationale Contre le Cancer - Conseil Scientifique Inter Régional Grand Ouest; the Association CANCEN; the Ministère de la Recherche et des Technologies; the Institut National de la Santé et de la Recherche Médicale (INSERM); the Région Centre. Ligue Nationale Contre le Cancer – Comité National (B.J.); University of Tours in 2010 (L.-H.J.).

Acknowledgements

We thank Isabelle Domingo and Catherine Le Roy for technical and administrative assistance, respectively. We thank Prof. Alan R.North (University of

Manchester, UK) for the generous gift of plasmids encoding the human P2X receptors.

Conflict of Interest Statement: None declared.

References

1. Parkin,D.M. *et al.* (2005) Global cancer statistics, 2002. *CA. Cancer J. Clin.,* **55**, 74–108.
2. Gupta,G.P. *et al.* (2006) Cancer metastasis: building a framework. *Cell*, **127**, 679–695.
3. Burnstock,G. (2006) Purinergic signalling. *Br. J. Pharmacol.,* **147** (suppl. 1), S172–S181.
4. Pellegatti,P. *et al.* (2008) Increased level of extracellular ATP at tumor sites: in vivo imaging with plasma membrane luciferase. *PLoS ONE*, **3**, e2599.
5. Raffaghello,L. *et al.* (2006) The P2X7 receptor sustains the growth of human neuroblastoma cells through a substance P-dependent mechanism. *Cancer Res.,* **66**, 907–914.
6. Wang,X. *et al.* (2004) P2X7 receptor inhibition improves recovery after spinal cord injury. *Nat. Med.,* **10**, 821–827.
7. White,N. *et al.* (2006) P2 receptors and cancer. *Trends Pharmacol. Sci.,* **27**, 211–217.
8. Roger,S. *et al.* (2011) P2X7 receptor antagonism in the treatment of cancers. *Expert Opin. Investig. Drugs*, **20**, 875–880.
9. Rassendren,F. *et al.* (1997) The permeabilizing ATP receptor, P2X7. Cloning and expression of a human cDNA. *J. Biol. Chem*., **272**, 5482–5486.
10. North,R.A. (2002) Molecular physiology of P2X receptors. *Physiol. Rev*., **82**, 1013–1067.
11. Roger,S. *et al.* (2008) Facilitation of P2X7 receptor currents and membrane blebbing via constitutive and dynamic calmodulin binding. *J. Neurosci*., **28**, 6393–6401.
12. Roger,S. *et al.* (2010) C-terminal calmodulin-binding motif differentially controls human and rat P2X7 receptor current facilitation. *J. Biol. Chem*., **285**, 17514–17524.
13. Surprenant,A. *et al.* (1996) The cytolytic P2Z receptor for extracellular ATP identified as a P2X receptor (P2X7). *Science*, **272**, 735–738.
14. Di Virgilio,F. *et al.* (1998) Cytolytic P2X purinoceptors. *Cell Death Differ*., **5**, 191–199.
15. Surprenant,A. *et al.* (2009) Signaling at purinergic P2X receptors. *Annu. Rev. Physiol*., **71**, 333–359.
16. Di Virgilio,F. (2007) Liaisons dangereuses: P2X(7) and the inflammasome. *Trends Pharmacol. Sci*., **28**, 465–472.
17. Barberà-Cremades,M. *et al.* (2012) P2X7 receptor-stimulation causes fever via PGE2 and IL-1β release. *FASEB J.*, **26**, 2951–2962.
18. Pelegrin,P. (2008) Targeting interleukin-1 signaling in chronic inflammation: focus on P2X(7) receptor and Pannexin-1. *Drug News Perspect*., **21**, 424–433.
19. Adinolfi,E. *et al.* (2002) P2X7 receptor expression in evolutive and indolent forms of chronic B lymphocytic leukemia. *Blood*, **99**, 706–708.
20. Wang,Q. *et al.* (2004) P2X7 receptor-mediated apoptosis of human cervical epithelial cells. *Am. J. Physiol. Cell Physiol*., **287**, C1349–C1358.
21. Zhang,X.J. *et al.* (2004) Expression of P2X7 in human hematopoietic cell lines and leukemia patients. *Leuk. Res*., **28**, 1313–1322.
22. Slater,M. *et al.* (2004) Differentiation between cancerous and normal hyperplastic lobules in breast lesions. *Breast Cancer Res. Treat*., **83**, 1–10.
23. Slater,M. *et al.* (2004) Early prostate cancer detected using expression of non-functional cytolytic P2X7 receptors. *Histopathology*, **44**, 206–215.
24. Deli,T. *et al.* (2007) Functional genomics of calcium channels in human melanoma cells. *Int. J. Cancer*, **121**, 55–65.
25. Solini,A. *et al.* (2008) Increased P2X7 receptor expression and function in thyroid papillary cancer: a new potential marker of the disease? *Endocrinology*, **149**, 389–396.
26. Slater,M. *et al.* (2005) Expression of the apoptotic calcium channel P2X7 in the glandular epithelium. *J. Mol. Histol*., **36**, 159–165.
27. Di Virgilio,F. *et al.* (2009) P2X(7): a growth-promoting receptor-implications for cancer. *Purinergic Signal*., **5**, 251–256.
28. Adinolfi,E. *et al.* (2012) Expression of P2X7 receptor increases *in vivo* tumor growth. *Cancer Res*., **72**, 2957–2969.
29. Jelassi,B. *et al.* (2011) P2X(7) receptor activation enhances SK3 channels- and cystein cathepsin-dependent cancer cells invasiveness. *Oncogene*, **30**, 2108–2122.
30. Huang,H.C. *et al.* (1991) Vasorelaxants from Chinese herbs, emodin and scoparone, possess immunosuppressive properties. *Eur. J. Pharmacol*., **198**, 211–213.
31. Koyama,M. *et al.* (1988) Novel type of potential anticancer agents derived from chrysophanol and emodin. Some structure-activity relationship studies. *J. Med. Chem*., **31**, 283–284.
32. Tabolacci,C. *et al.* (2010) Antitumor properties of aloe-emodin and induction of transglutaminase 2 activity in B16-F10 melanoma cells. *Life Sci*., **87**, 316–324.
33. Chen,Y.Y. *et al.* (2010) Emodin, aloe-emodin and rhein inhibit migration and invasion in human tongue cancer SCC-4 cells through the inhibition of gene expression of matrix metalloproteinase-9. *Int. J. Oncol*., **36**, 1113–1120.
34. Liu,L. *et al.* (2010) Inhibition of ATP-induced macrophage death by emodin via antagonizing P2X7 receptor. *Eur. J. Pharmacol*., **640**, 15–19.
35. Gillet,L. *et al.* (2009) Voltage-gated sodium channel activity promotes cysteine cathepsin-dependent invasiveness and colony growth of human cancer cells. *J. Biol. Chem*., **284**, 8680–8691.
36. Brisson,L. *et al.* (2011) Na(V)1.5 enhances breast cancer cell invasiveness by increasing NHE1-dependent H(+) efflux in caveolae. *Oncogene*, **30**, 2070–2076.
37. Donnelly-Roberts,D.L. *et al.* (2007) Discovery of P2X7 receptor-selective antagonists offers new insights into P2X7 receptor function and indicates a role in chronic pain states. *Br. J. Pharmacol*., **151**, 571–579.
38. Egeblad,M. *et al.* (2002) New functions for the matrix metalloproteinases in cancer progression. *Nat. Rev. Cancer*, **2**, 161–174.
39. Mohamed,M.M. *et al.* (2006) Cysteine cathepsins: multifunctional enzymes in cancer. *Nat. Rev. Cancer*, **6**, 764–775.
40. Marques,I.J. *et al.* (2009) Metastatic behaviour of primary human tumours in a zebrafish xenotransplantation model. *BMC Cancer*, **9**, 128.
41. Li,X. *et al.* (2006) The P2X7 receptor: a novel biomarker of uterine epithelial cancers. *Cancer Epidemiol. Biomarkers Prev*., **15**, 1906–1913.
42. Adinolfi,E. *et al.* (2005) Basal activation of the P2X7 ATP receptor elevates mitochondrial calcium and potential, increases cellular ATP levels, and promotes serum-independent growth. *Mol. Biol. Cell*, **16**, 3260–3272.
43. Gu,L.Q. *et al.* (2010) Association of XIAP and P2X7 receptor expression with lymph node metastasis in papillary thyroid carcinoma. *Endocrine*, **38**, 276–282.
44. Ren,S. *et al.* (2010) Targeting $P2X_7$ receptor inhibits the metastasis of murine P388D1 lymphoid neoplasm cells to lymph nodes. *Cell Biol. Int*., **34**, 1205–1211.
45. Ralevic,V. *et al.* (1998) Receptors for purines and pyrimidines. *Pharmacol. Rev*., **50**, 413–492.
46. Böhme,H.J. *et al.* (1972) Affinity chromatography of phosphofructokinase using Cibacron blue F3G-A. *J. Chromatogr*., **69**, 209–214.
47. Baqi,Y. *et al.* (2010) Synthesis of alkyl- and aryl-amino-substituted anthraquinone derivatives by microwave-assisted copper(0)-catalyzed Ullmann coupling reactions. *Nat. Protoc*., **5**, 945–953.

Received July 27, 2012; revised February 11, 2013; accepted March 8, 2013